

# Precipitation Kinetics and Transformation of Metastable Phases in Al-Mg-Si Alloys

*Al-Mg-Si precipitation-hardening alloys are much used in the aerospace and automotive industries, owing to the combined merits of low weight and strong mechanical properties. The mechanical properties of the alloys are mainly contributed to the metastable precipitate phases formed during artificial aging. Although numerous investigations using transmission electronic microscopy (TEM) and differential scanning calorimetry (DSC) have been conducted for the nanostructural characterization and precipitation behaviors of precipitates in Al-Mg-Si alloys, the understanding of precipitation is incomplete and limited. In situ synchrotron small-angle X-ray scattering (SAXS) reported here is the first SAXS study on the temporal evolution of metastable precipitate structures in different Al-Mg-Si alloys, including radius, length, and volume fraction. The present study demonstrates the precipitation and transformation behaviors of metastable  $\beta''$  and  $\beta'$  phases of the naturally aged Al-Mg-Si alloys during continuous heating, and subsequently isothermal aging. A new SAXS analysis approach for the complex SAXS profiles enabled a quantitative analysis on the structural evolution and the corresponding kinetics of the concurrent needle-like  $\beta''$  and rod-like  $\beta'$  phase transformations.*

## Beamline

01B1 X-ray Microscopy

## Authors

C.-S. Tsao and C.-Y. Chen  
Institute of Nuclear Energy  
Research, Longtan, Taiwan

U.-S. Jeng  
National Synchrotron Radiation  
Research Center, Hsinchu,  
Taiwan

T.-Y. Kuo  
Southern Taiwan University of  
Technology, Tainan, Taiwan

 **In** the investigation of nanostructural evolution of a large number of particles in a bulk sample with heat-treatment time, in situ SAXS is shown as a powerful tool compared to the inherent drawbacks of TEM technique. Because the SAXS contrast between  $\beta''$  (or  $\beta'$ ) precipitates, MgSi, and matrix Al is very low, no SAXS study on the structural evolution of  $\beta''$  precipitates has been reported. In the present study, we perform SAXS for an Al-Mg-Si alloy with high flux and high-energy photons from synchrotron radiation. The penetration of 15 keV photons selected allows an optimum SAXS sample thickness of the alloys five folds thicker than that with 8 keV photons. Therefore, the scattering intensity from  $\beta''$  precipitates in the Al matrix can be further enhanced by the same factor. The high flux together with the larger optimum sample thickness  $\sim 0.5$  mm facilitated successfully the in situ SAXS investigation for the precipitation behavior of the naturally aged Al-Mg-Si alloy during artificial aging. Similar to the general studies about Al-Mg-Si alloys, two artificial aging temperatures of interest:  $\sim 180^\circ\text{C}$  for  $\beta''$  precipitates, and  $\sim 260^\circ\text{C}$  for  $\beta'$  as well as  $\beta''$  precipitates were focused on here. We performed in situ SAXS for both Al-Mg-Si alloys, AA6022 (typical Al-Mg-Si ternary alloy) and AA6111 (Al-Mg-Si alloys containing Cu, quaternary alloy).

In the present study using in situ synchrotron SAXS technique, the time-dependent SAXS profiles measured can be characterized by two regimes: the  $Q > 0.04 \text{ \AA}^{-1}$  regime contributed by needle-like  $\beta''$  precipitates of a typical radius of  $\sim 3$  nm and the  $Q < 0.04 \text{ \AA}^{-1}$  regime dominated by rod-like  $\beta'$  precipitates of a typical radius of  $\sim 10$  nm. Due to the substantial difference in size, the two scattering contributions by  $\beta''$  and  $\beta'$  precipitates can be separated relatively well from the SAXS profiles for a quantita-

tive analysis of the structural evolutions of the two concurrent  $\beta''$  and  $\beta'$  phase transformations. The corresponding precipitation and dissolution kinetics for each precipitate phase are quantitatively established.

The structural evolution and precipitation kinetics of  $\beta''$  and  $\beta'$  phases during continuous heating from room temperature (RT) to 260°C are depicted in the time-dependent SAXS profiles measured (see Fig. 1). The SAXS profiles measured during continuous heating from RT to 211°C were nearly the same, indicating no observable structural change (incubation period). During 211°C–260°C in the heating process, the SAXS profiles intensities increase with the temperature in the intermediate- to high- $Q$  region ( $Q \geq 0.05 \text{ \AA}^{-1}$ ), indicating a nucleation and growth of  $\beta''$  precipitates. Above 235°C, the SAXS profile intensity in the low- $Q$  region, dominated by newly formed large precipitates, increases with temperature and aging time, and changes gradually from the behavior of  $I(Q) \propto Q^{-4}$  (at RT) to  $I(Q) \propto Q^{-2.1}$ . The transition of the scattering characteristics is mainly due to the nucleation and growth of the rod-like  $\beta'$  precipitates of a much larger size than the  $\beta''$  precipitates formed concurrently. The model-fitted length of  $\beta''$  precipitates increases largely during the heating process from 18.3 nm at 211~235°C to 150 nm at 235~260°C. Note that the temporal evolution of the model-fitted values for the  $\beta''$  precipitates reveals an inert radius (around 3.1 nm) and a rapid growing length with aging time. The structural evolutions of  $\beta''$  and  $\beta'$  precipitates during the continuous heating in terms of model-fitted size and volume fraction can be characterized by the early stage of a typical precipitation, i.e., the concomitant nucleation and growth.

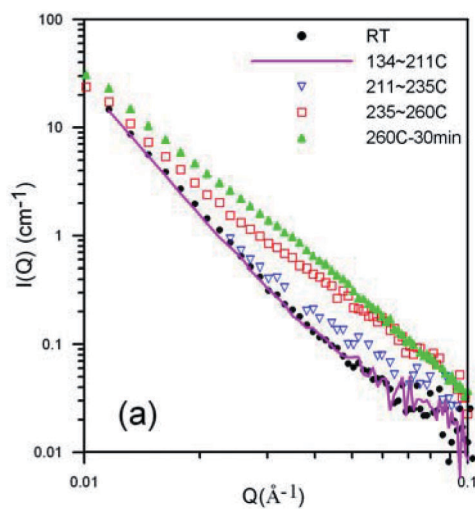


**Fig. 1:** Selected time-dependent SAXS profiles measured for the naturally aged alloy AA6022 during continuous heating from RT to 260°C, together with that obtained during subsequent isothermal artificial aging at 260°C for 30 min.

Phase transformation kinetics of  $\beta''$  concurrent with  $\beta'$  phases during isothermal aging at 260°C are revealed by the corresponding time-dependent SAXS profiles measured. The structural parameters obtained from the model-fitting are in good agreement with the result extracted from model-independent Kratky-Porod approximations in the different  $Q$  regions corresponding to the  $\beta''$  and  $\beta'$  regimes. The stable cross-section and rapid length growth along the needles of  $\beta''$  phase, and the radius growth of  $\beta'$  phase during the temporal evolution of isothermal aging were characterized well by the concomitant nucleation, growth and coarsening stages. From the beginning of the isothermal aging, the rapidly growing radius and volume fraction of  $\beta'$  precipitates with aging time still exhibit a typical nucleation and growth behavior (see Fig. 2). After  $t = 210$  min, the radius and volume fraction evolutions of  $\beta'$  precipitates with aging time change to a typical behavior of coarsening. The volume fraction of the  $\beta''$  precipitates remains in the nucleation and growth step during the continuous heating, and reaches their peak value 30 min after the isothermal aging at 260°C. Thereafter, the volume fraction of  $\beta''$  precipitates starts to decrease significantly with the aging time, and at  $t = 510$  min, saturates at a value of 65 % of the maximum volume fraction. Our in situ SAXS result reveals that 35% of the  $\beta''$  phase can be consumed by dissolution and/or transformation ( $\beta'' \rightarrow \beta'$  precipitates) within 8 hr of isothermal aging, and then remain a constant volume fraction. The rapid nucleation and growth of  $\beta'$  phase is concurrent with the significant dissolution of  $\beta''$  phase during  $t = 30$  min~ 210 min. In principle, the sites of dissolved  $\beta''$  precipitates are also more favored as

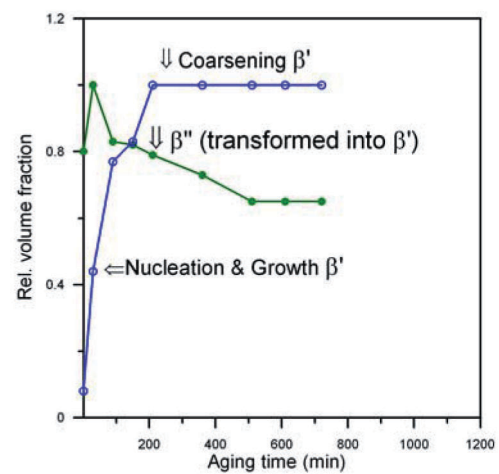


**Fig. 2:** Comparison of the temporal evolutions of volume fractions of  $\beta''$  concurrent with  $\beta'$  phases in AA6022 alloy aged at 260°C, demonstrating the typical precipitation and partial dissolution for each phase.

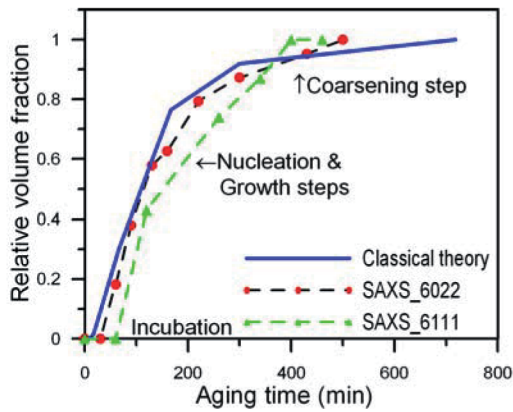


**Fig. 3:** Comparison of temporal evolutions of volume fractions of  $\beta''$  precipitates determined from the SAXS analysis for AA6022 and AA6111 alloys aged at 180°C, with that predicted by numerical simulation based on classical theory.

the nucleation sites of  $\beta'$  precipitates. Our TEM examination for the SAXS specimen shows the consistent result on the morphology and coexistence of needle-like  $\beta''$  and rod-like  $\beta'$  precipitates.

This study also compares the structural evolution and the precipitation kinetics of  $\beta''$  precipitates in AA 6111 and 6022 alloys isothermally aged at 180°C (typical  $\beta''$  precipitation temperature), taking into account the effect of solute Mg and Cu contents. The mean radius of  $\beta''$  precipitates, 1.78 nm, determined by model fitting for the AA 6111 alloy is smaller than that for the AA6022 alloy, 2.77 nm. The smaller radius for the AA 6111 alloy can be attributed to the reduced solute atoms due to more natural aging clusters formed. The structural evolution of the precipitates in both alloys exhibits an inert radius and a growth in length with aging time. Figure 3 compares the temporal evolutions of the relative volume fractions of  $\beta''$  precipitates in both AA 6022 and AA 6111 alloys obtained by SAXS model fitting, with that for the Al-0.63%Mg-Si alloy obtained by the numerical simulation based on the classical model. The numerical simulation was based on artificial aging at 180°C without natural aging treatment. All temporal evolutions presented in Fig. 3 are characterized effectively by coupled nucleation, growth and coarsening. The SAXS results of both alloys clearly indicate the incubation period associated with the natural aging effect. The incubation period of AA 6111 alloy, ~60 min, exceeds that of A 6022 alloy, ~30 min, because the former alloy has a higher MgSi content, leading to the more natural clusters.

### Experimental Station

Small-angle X-ray scattering station

### Publications

- C.-S. Tsao, C.-Y. Chen and J.-Y. Huang, *Phys. Rev. B* **70**, 174104 (2004).
- C.-S. Tsao, U-S. Jeng, C.-Y. Chen and T.-Y. Kuo, *Scripta Mater.* **53**, 1241 (2005).
- C.-S. Tsao, C.-Y. Chen, U-S. Jeng, and T.-Y. Kuo, *Acta Mater.* **54**, 4621 (2006).

### Contact E-mail

cstsao@iner.gov.tw